

# Measurement of the Spin of the M87 Black Hole from its Observed Twisted Light

Fabrizio Tamburini,<sup>1,\*</sup> Bo Thidé,<sup>2,†</sup> and Massimo Della Valle<sup>3,‡</sup>

<sup>1</sup>ZKM, Lorenzstraße 19, Karlsruhe, D-76135 Germany

<sup>2</sup>Swedish Institute of Space Physics, Ångström Laboratory, Box 537, SE-751 21 Uppsala, Sweden

<sup>3</sup>Capodimonte Astronomical Observatory, INAF-Napoli, Salita Moiariello 16, I-80131 Naples, Italy

We present observational evidence that light propagating near a rotating black hole is twisted, *i.e.*, carries orbital angular momentum (OAM). Using wavefront reconstruction and phase recovery techniques, we extracted the OAM spectra from  $\lambda = 1.3$  mm radio intensity data collected by the Event Horizon Telescope from around the black hole M87\*. The twisted-light/OAM method, complementary to black-hole shadow circularity analysis, allows a direct probing of Kerr metrics and shows that the M87\* rotates clockwise with an estimated rotation parameter  $a \sim 0.9 \pm 0.1$ .

Keywords:

Most of the knowledge we have about the Universe comes from observing and interpreting its electromagnetic (EM) radiation. The information carried by the EM field is encoded, naturally or artificially, into conserved quantities (observables) of the field that are transported from the source to the distant observer where the information can be decoded and recovered. The standard observables are the well-known ten conserved quantities that are concomitant with the ten-dimensional Poincaré group of Noether invariants: the field energy, used in, *e.g.* radiometry, linear momentum, used in, *e.g.* radio communications, angular momentum, used only partially in radio science and technology, and the center of energy. Of these quantities, the angular momentum, connected with rotation and torque action [1], has not yet been fully exploited in astronomy [2–4]. Only the spin angular momentum (SAM) associated with photon helicity, *i.e.*, the wave polarization, has been utilized so far.

Light and radio emitted from near a massive rotating black hole are expected to be endowed with orbital angular momentum (OAM) [5], by the fact that superpositions of photon eigenstates, each with a well-defined value of SAM and OAM [6], form near a rotating black hole due to general relativity (GR) effects such as Kerr spacetime dragging and mixing, and gravitational lensing. Here we present the first observational evidence of such GR induced vorticity, extracted from public brightness temperature data [7] from Event Horizon Telescope (EHT) observations at  $\lambda = 1.3$  mm of the central compact radio source surrounding a supermassive black hole M87\* in the Virgo Cluster galaxy M87 [8–13]. Exploiting this vorticity we were able to directly probe the Kerr metric of the M87\* by measuring its spin, its sense of rotation, and its inclination, as reported in this Letter.

Twisted beams can be decomposed into orthogonal eigenmodes, each carrying its own well-defined quantum of OAM and known geometry. A convenient choice is Laguerre-Gaussian modes. In cylindrical polar coordinates  $(\rho, \varphi, z)$  these paraxially approximate modes describe an EM field at  $z = 0$  with amplitude [14]

$$U_{m,p}^{\text{L-G}}(r, \varphi, 0) \propto R(\rho) \exp(im\varphi), \quad m = 0, \pm 1, \pm 2, \dots \quad (1a)$$

where

$$R(\rho) = \left( \frac{\sqrt{2}\rho}{w(0)} \right)^m L_p^m \left( \frac{2\rho^2}{w^2(0)} \right) \quad (1b)$$

The parameter  $m$  is the azimuthal index that describes the  $z$  component of OAM, *i.e.* the number of twists present in the helical wavefront,  $p$  is the radial node number of the mode,  $w(z)$  the waist of the beam,  $L_p^m$  the associated Laguerre orthogonal polynomial, and  $\varphi$  the azimuthal phase of the beam<sup>19,20</sup>. The decomposition of any general beam into orthogonal modes will expose the spectrum of OAM states carried by the EM wavefront, the so called spiral spectrum [15]. As is seen from (1), this spectrum of OAM states carried by the EM wavefront is obtained by Fourier transforming the EM field with respect to the azimuthal angle  $\varphi$ . Since the twisted-light/OAM method operates in angular momentum space it is complementary to methods based on analyses in configuration ( $\varphi$ ) space, such as the analysis of the deviation from the circularity of the M87\* shadow, a method that has so far not been able to yield any conclusive results [8–13, 16]. The EHT observations were made at 1.3 mm wavelength to generate the spatial phase distribution of the EM field and provide an estimate of the OAM spectral content in the lensed light.

As has been demonstrated experimentally in the radio domain [17–19], vortex beams are detectable and can be accurately characterized by means of interferometric techniques. In our case, however, we employ instead a non-interferometric technique that amounts to the measurement of the vortex beam wavefront based on the Transport-of-Intensity Equation (TIE) method and reduced error procedure [20–24] on the four intensity images of the Einstein ring of M87\* taken in radio at 1.3 mm [7], benefiting from the fact that the Earth and the M87\* are in relative motion.

This allowed us to obtain the OAM spectrum (spiral spectrum) of the received radio light, thus confirming the predictions made in Ref. 5. Furthermore, from the asymmetry of the observed OAM spectrum we were able to determine the sense and magnitude of the rotation of the M87\* and its inclination.

In fact, in Kerr metric [25], the geometry of the shadow and the radius of the photon ring, the photon capture radius, relative to that of a Schwarzschild BH, changes with the ray orientation relative to the angular momentum vectors. This results in a deformation of the circular shape of the black hole's shadow. This deformation, even if it is small ( $< 4\%$ ), can be potentially detectable only with future EHT acquisitions [8] that allow the determination of the inclination of the BH spin and the presence of a clockwise rotation from the comparison of the data with about 60,000 templates obtained from numerical simulations involving the BH surroundings and the shadow that is nearly circular with an expected maximum asymmetry of  $\leq 10\%$  in the most prominent cases. The OAM method, on the other hand, does not depend directly on the asymmetry of the BH shadow. Instead, it makes use of the vorticity induced by the Kerr metric and emitted by a slightly larger region of the Einstein ring surrounding the BH.

In contrast to the EHT approach to determine the rotation of the M87\*, our approach is to reconstruct the evolution of the wavefront from two sets of two consecutive images separated by one day each, taken on 5 April and 6 April 2017, and on 10 April and 11 April 2017, respectively. With this method one can reconstruct the spatial phase distribution and estimate the OAM content in the images that depends on the rotation parameters obtained from the two different acquisitions.

As an initial step in the analysis and interpretation of the EHT data, we built up, from a set of numerical simulations, several scenarios of black-hole accretion disks to use as a catalog of reference models to be compared with the results from the experimental data analysis, allowing us to characterize the twisting of light from the rotating BH of M87. To this end we solved numerically the null geodesic equations under strong gravity conditions with the help of the freely available software package KERTAP [26] that provides a detailed description of the propagation of light in Kerr spacetime [25] in geometric units ( $G = c = 1$ ) with an error on the order of  $10^{-7}$ .

The OAM of the light from the M87\* Einstein ring was calculated from the Stokes polarization parameters [27] as measured by an ideal asymptotic observer. Because of the properties of the Kerr metric, the observables associated with any Kerr black hole (KBH), including the spatial distribution of the azimuthal photon phase  $\phi(\varphi)$  and the associated OAM spiral spectrum considered here, are invariant with respect to the mass  $m_{\text{BH}}$  of the BH but depend on its rotation parameter  $a = J_{\text{BH}}/(m_{\text{BH}}c)$ , where  $J_{\text{BH}}$  is the BH angular momentum, and the inclination  $i$  of its equatorial plane with respect to the observer. In all our simulations we assumed  $0.5 < a < 0.99$  and  $1^\circ < i < 179^\circ$ , rotating clockwise and counterclockwise, then favoring  $i = 17^\circ$  rotating clockwise and pointing away from Earth with the angular momentum of the accretion flow and that of the BH anti-aligned, or equivalent to  $i = 163^\circ$  with the angular momenta of the accretion flow and that of the BH aligned, as discussed in Ref. 12, for a magnetically arrested disk [28], as indicated by the spiral spectra obtained from the experimental data and from the results of the EHT collaboration, presented and discussed in Refs. 8, 9, 10, 11, 12 and 13.

To determine the OAM of the light from the Stokes parameters and the Pancharatnam-Berry phase generated by the KBH lensing we considered the electric field of a fully polarized vectorial vortex beam propagating in free space in the  $z$  direction from the BH to the asymptotic observer. In the paraxial approximation this field can be written [cf. Eqn. (1.5) in Ref. 29]

$$\mathbf{E}(x,y) = i\omega \left[ u_x \hat{\mathbf{x}} + u_y \hat{\mathbf{y}} + \frac{i}{k} \left( \frac{\partial u_x}{\partial x} + \frac{\partial u_y}{\partial y} \right) \hat{\mathbf{z}} \right] \exp(ikz) \quad (2)$$

where  $u_x$ ,  $u_y$ ,  $u_x^*$  and  $u_y^*$  represent the complex amplitudes of the  $x$  and  $y$  components and their complex conjugates, respectively, of the electric field in the image plane,  $\omega$  is the angular frequency, and  $k$  the wave number.

In SI units the  $z$  component of the EM orbital angular momentum density about the origin is [30]

$$\epsilon_0 [\mathbf{x} \times (\mathbf{E} \times \mathbf{B})] \cdot \hat{\mathbf{z}} = \frac{\epsilon_0}{2\omega} \sum_{i=1}^3 E_i^* \hat{L}_z E_i = \frac{\epsilon_0}{2\omega} \sum_{i=1}^3 E_i^* \left( -i \frac{\partial}{\partial \varphi} \right) E_i$$

so that one obtains [27]

$$\hat{L}_z = i \frac{\omega}{2} \left( u_x \frac{\partial u_x^*}{\partial \varphi} + u_y \frac{\partial u_y^*}{\partial \varphi} - u_x^* \frac{\partial}{\partial \varphi} - u_y^* \frac{\partial}{\partial \varphi} \right) \quad (3)$$

From the Stokes parameters ( $I, U, V$ ), the Pancharatnam phase of the vortex field  $\mathbf{E}(x,y)$  that we want to determine is given by [27]

$$\psi_{P(V/U)} = \arg(\langle \Phi_V | \Phi_E \rangle) \quad (4)$$

More precisely, this quantity is calculated with the argument of the ratio between the circular/elliptic state of polarization of the EM field, characterized by the Stokes parameter  $V$ , and state  $|\Phi_V\rangle$ , and that of the initial field  $\mathbf{E}(x,y)$ , namely  $|\Phi_E\rangle$ .

Then [27], one obtains the average OAM charge of the field, for any concentric circle of pixels with the origin in the center of the image with radius  $r_c$ , from

$$\frac{\partial m}{\partial \phi} = r_c I_N \left( -I \frac{\partial \psi_{P(V/U)}}{\partial \phi} \mp (I \pm U) \frac{\partial \psi_s}{\partial \phi} \right) \quad (5)$$

where the  $I_N$  is the normalized intensity, and the first term  $I \partial(\psi_{P(V/U)})/\partial \phi$  is the gradient of the spiral spatial phase distribution obtained from the Stokes parameters  $V$  and  $U$ . The term  $(I \pm U) \partial \psi_s / \partial \phi$  in Eqn. (5) describes the variation of the state of polarization in space at each point in the observational plane of an asymptotic observer.

In the reconstruction of the spatial phase distribution from the intensity of the field, the EM waves are described by complex-valued solutions  $u(r)$  of the paraxial wave equation [23, 31]

$$\left( \nabla_{(x,y)} \cdot \nabla_{(x,y)} + 4\pi i \frac{\partial}{\partial z} \right) u(r) = 0 \quad (6)$$

where  $\nabla_{(x,y)}$  represents the vector nabla differential operator in the image plane  $(x,y)$  perpendicular to the  $z$  axis connecting the BH and the asymptotic observer.

By multiplying equation (6) with its complex conjugate, one can split the equation into a system of partial differential equations describing the intensity  $I$  (the TIE equation) and the phase evolution  $P$  with respect a motion across the  $z$  axis as in Ref. 23

$$\frac{\partial I}{\partial z} = -\frac{1}{2\pi} \nabla_{(x,y)} \cdot (I \nabla_{(x,y)} P) \quad (7a)$$

$$\frac{\partial P}{\partial z} = \frac{1}{4\pi\sqrt{I}} \nabla_{(x,y)}^2 \sqrt{I} - |\nabla_{(x,y)} P|^2 \quad (7b)$$

where  $I$  is the intensity and  $P$  the phase distributions in the plane of propagation that evolves along the  $z$  coordinate. The quantity  $|\nabla_{(x,y)} P|$  is the magnitude of the phase gradient vector in the image plane.

To solve the equation system (7) and recover the spatial phase distribution, and thus the OAM imprinted in the experimental data, we split the four observations into two subgroups of two images each, separated by a one day interval. This was done in order to reduce any influence on the procedure due to possible actual physical changes in the Einstein ring for a KBH supposed to rotate near the maximum rate. We found that during these time intervals the stability of the source does not exhibit dramatic structural changes, as already stated in Refs. 12 and 32.

M87\* presents a modest source evolution between the two pairs of nights 5–6 April and 10–11 April and a broad consistency within each pair. The evolution of the source during the time interval between the two sets of pairs of days, was  $< 5\%$  within an observation [10, 11].

Also, the evolution of  $P$  and  $I$  along the  $z$  axis expressed in Eqns. (7) is provided by the motion of the Earth during the acquisitions. The TIE equation can be applied even though the shift along  $z$  due to the motion of our planet around the Sun in the interval of one day appears to be enormous with respect to the wavelength. However, this method still applies as this motion represents a fairly small fraction of the distance traveled by light from M87\* to the Earth and because of the stability of propagation of the light so far observed and the slow evolution of the source during the acquisition time interval.

The evolution of the M87\* Einstein ring structure during the two different EHT observation runs (epoch 1 and epoch 2) in two 2 GHz frequency bands centered on 227.1 GHz and 229.1 GHz (for more details see Ref. 7, 13), each separated by one day, is negligible. This can be taken as evidence that only higher-order, small perturbations are present in the spiral spectrum.

Relative to the object, each day is  $2.8R_g c^{-1}$  long for a BH with mass  $M = 6.5 \pm 0.2|_{\text{stat}} \pm 0.7|_{\text{sys}} \times 10^9 M_\odot$ . This timescale is shorter than the crossing time of light of the source plasma and short compared to the decorrelation timescale of EHT simulations used to analyze the experimental results [12],  $50R_g c^{-1}$ .

This is the reason why we chose to estimate the OAM from the asymmetry parameter  $q$  of the OAM spectrum components  $\ell = 1$  and  $\ell = -1$  only. If  $q > 1$ , then the rotation is clockwise, whilst  $q = 1$  indicates no rotation and  $q < 1$  counterclockwise rotation [1]. The rotation parameter,  $a$ , can be calculated from the asymmetries present in the experimental and theoretical spiral spectra. The value of  $a$  was estimated from the experimental data from two different runs, each separated by one day, the first being epoch 1 (5 and 6 April 2017), and the second being epoch 2 (10 and 11 April 2017). The data were obtained from 10 seconds of signal averaging as described in Refs. 11, 12, and 13. The imaging techniques applied to this data set reveal the presence of an asymmetric ring with clockwise rotation and a ‘‘crescent’’ geometric structure that exhibits a clear central brightness depression. This indicates a source dominated by lensed emission surrounding the black hole shadow.

From the analysis of the two data sets we obtain the asymmetry parameters  $q_1 = 1.417$  for epoch 1 and  $q_2 = 1.369$  for epoch 2. They yield an averaged asymmetry in the spiral spectrum of  $\bar{q} = 1.393 \pm 0.024$  in agreement with that of our numerical simulations, such as  $q_{\text{num}} = 1.375$ , of an Einstein ring with a radius of 5 gravitational radii, emitting partially incoherent light

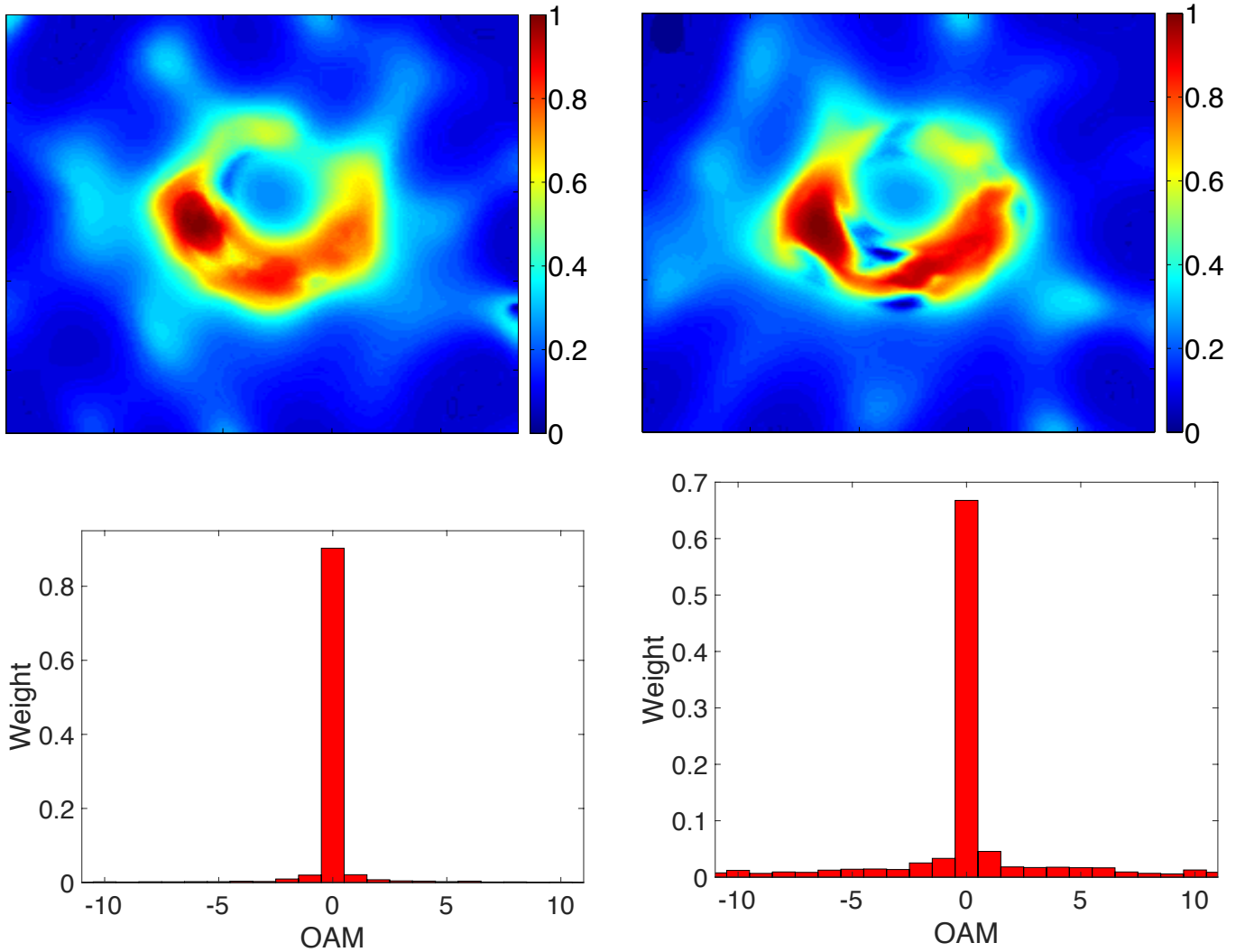


Figure 1: **Experimental results.** Normalized electric field component magnitudes along the observer’s direction reconstructed from the TIE analysis of the brightness temperature for the corresponding spiral spectra for epoch 1 and epoch 2. The asymmetry between the  $\ell = 1$  and  $\ell = -1$  components in both of the spiral spectra reveals twisted lensing of a black hole [5] with  $a = 0.9 \pm 0.1$  rotating clockwise and the spin pointing away from Earth and an inclination between the approaching jet and the line of sight of  $i = 17^\circ$  if the angular momentum of the accretion flow and that of the black hole are anti-aligned (equivalent to a similar geometry with an inclination  $i = 163^\circ$ , but where the angular momentum of the accretion flow and that of the BH are aligned). The Einstein ring has gravitational radius  $r = 5R_g$  dominated by incoherent emission. For all days, the diameters of the ring features span the narrow angular range 38–44  $\mu\text{s}$  and the observed peak brightness temperature of the ring is  $T \sim 6 \times 10^9 \text{ K}$  [7, 13].

Table I: Asymmetry ratio from numerical simulations. Simulation of the asymmetry parameter  $q$  of the angular momentum states of Kerr black holes with different rotation parameters  $0.5 < a < 0.9$  and two sample inclinations  $i = 17^\circ$  and  $i = 46^\circ$  and clockwise rotation (with  $q > 1$ , see text), averaged over different emission mechanisms characterized by  $0.1 < \Gamma < 2$  power spectra.

| BH rotation parameter $a$                         | 0.5   | 0.6   | 0.8   | 0.9   |
|---|-------|-------|-------|-------|
| Asymmetry ratio<br>$q = h(\ell = 1)/h(\ell = -1)$ |       |       |       |       |
| $i = 17^\circ$                                    | 1.295 | 1.320 | 1.356 | 1.391 |
| $i = 46^\circ$                                    | 1.392 | 1.412 | 1.424 | 1.438 |

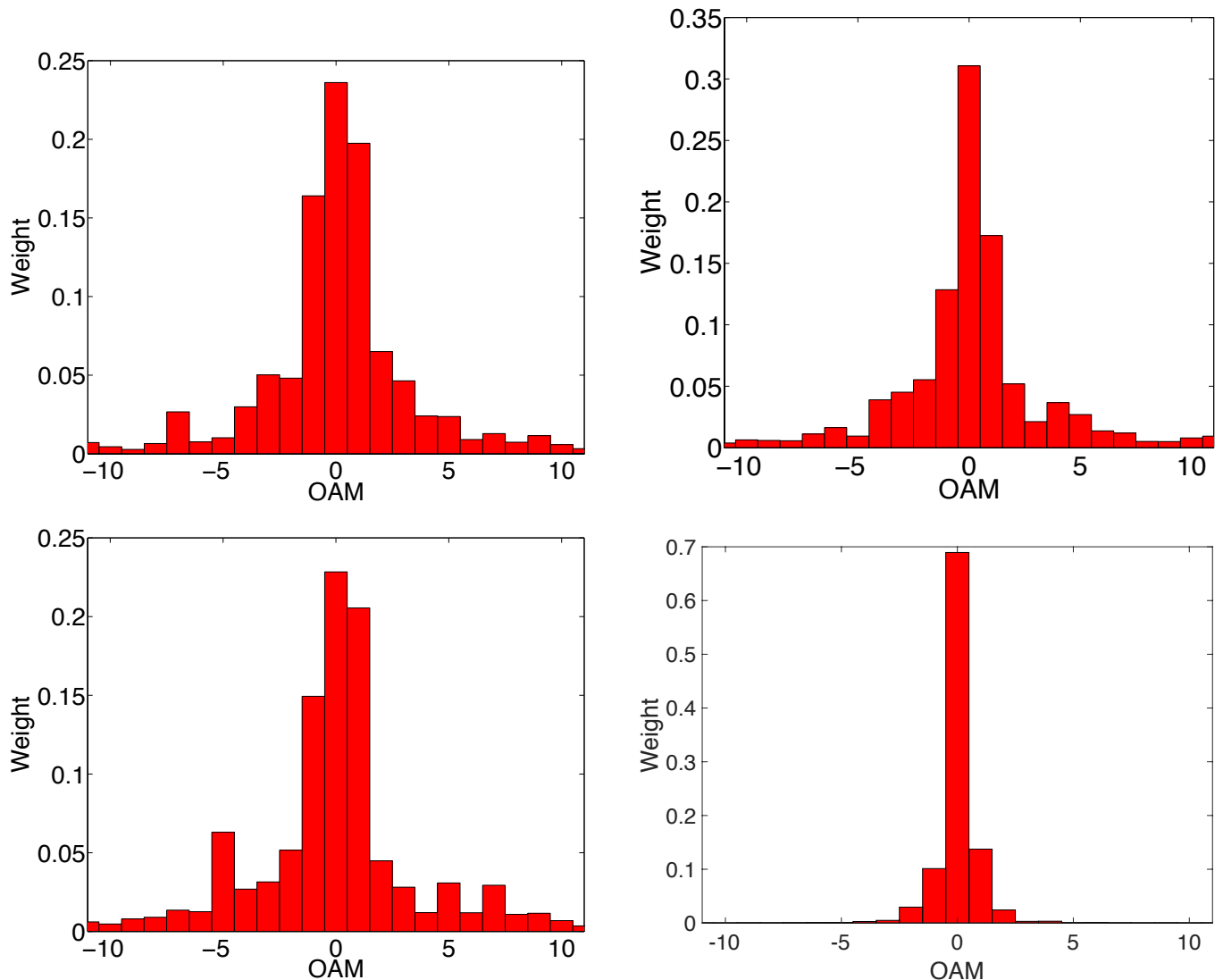


Figure 2: **Results from DIFMAP, EHT and SMILI data analyses and of numerical simulations from KERTAP.** *The first three insets show the experimental spiral spectra obtained from the three fiducial pipeline images for 11 April 2017 from SMILI, EHT imaging, and DIFMAP [7, 11, 13]. They represent the visibility amplitude and phase as a function of the vector baseline. In all the data sets the asymmetry parameter, the ratio between the  $\ell = 1$  and  $\ell = -1$  peaks in the spiral spectra, is  $q > 1$  indicating clockwise rotation as explained in Fig. 1. (left). Fourth inset: spiral spectrum of the numerical simulations with KERTAP is in agreement with the values found from these results and the TIE method [26].*

around a Kerr black hole with  $a \sim 0.9 \pm 0.1$ , corresponding to a rotational energy [33] of  $10^{64}$  erg, an energy that is comparable to the energy radiated by the brightest quasars over a Gyr timescale. The asymmetry parameters also yield an inclination  $i = 17^\circ$ , with the angular momenta of the accretion flow and of the black hole anti-aligned, showing clockwise rotation as described in Ref. 12, equivalent to a magnetically arrested disk (MAD) scenario with an inclination  $i = 163^\circ$  and the angular momentum of the accretion disk flow instead align with that of the black hole [28]. The X-ray luminosity is  $\langle L_X \rangle 10^{-2\sigma} < 4.4 \times 10^{40}$  erg/s and the jet power is  $P_{\text{jet}} > 10^{42}$  erg/s. The radiative efficiency is smaller than the corresponding thin disk efficiency [12].

Then one determines the rotation parameter  $a$  by comparing those obtained by a linear interpolation with the asymmetry parameter  $q$  of various models, as reported in the numerical example of Table for different values of inclination and rotation parameters  $i$  and  $a$ . The reconstructed fields and spiral spectra for the two epochs are reported in Figure 1.

Our results are in good agreement with results from an analysis of the fiducial pipeline images [7, 11, 13] of amplitude and phase plots for 11 April 2017 of DIFMAP with  $q = 1.401$ , of EHT with  $q = 1.361$  and of SMILI with  $q = 1.319$ , yielding for this day an averaged value of  $\bar{q} = 1.360$ . This value deviates by 0.09 from the epoch 2 value estimated with TIE, and  $q > 1$  confirms the clockwise rotation. The spiral spectra are reported in Figure 2. The TIE method requires coherent light to work at

full level. Even if the radio bandwidth is very narrow, The image reconstruction process together with the phase reconstruction of the wavefront used in the TIE method may introduce numerical noise and thus numerical decoherence in the spiral spectra. This is the reason why the ratios between the  $\ell = 0$  and  $\ell = \pm 1$  peaks obtained with TIE result in higher peaks than those present in the spiral spectra of the interferometric data.

In our simulations we adopted a thermalized emission with  $0.1 < \Gamma < 2$  power spectra, chosen in agreement with ALMA observations [12, 34] and also that of a synchrotron emission, Compton scattering, and bremsstrahlung. As discussed in Ref. 13, we find that, in any case, the image is determined mainly by the spacetime geometry and is also insensitive to the details of the plasma evolution between each observation in each of the two epochs.

Even if the spatial phase profile was not measured directly, something that can be achieved with interferometric or other more direct techniques, the values of the rotation parameter  $a$  obtained with the OAM method agrees with the experimental data obtained from results presented in the literature.

With dedicated observations and new interferometric methods that analyze the EM field in intensity and phase, one should be able to drastically improve the measurements of the OAM content in the EM radiation from rotating black holes. Ultimately, radio telescopes equipped with antenna systems optimized to directly capture and resolve the EM angular momentum in the signals received should be able to unleash the full potential of the OAM in observational astronomy.

One advantage of involving OAM in black-hole astronomy is that polarization and OAM together build up the total angular momentum invariant  $\mathbf{J}$  and when polarization is affected by the presence of polarizing media such as dust and unstructured plasma, OAM will be less affected and can be used as a reference point to extract additional information about the source from its emitted light.

We probed the Kerr metric of the M87\* by measuring its rotation. The estimate of the rotation parameter  $a$  was derived from the characterization of the vorticity of the electromagnetic waves emitted from the surroundings of the BH, affected by a strong gravitational lensing from the rotating compact object as discussed in Ref. 5. The electromagnetic vorticity was reconstructed from the public released images of the brightness temperature of the Einstein ring of the M87 black hole, taken during four different days with a well-known technique based on the Transport of Intensity Equation [22, 27, 35] that permits the reconstruction of the phase wavefront and of the orbital angular momentum content from two or more consecutive acquisitions of the same source taken at different distances. We find that the central black hole in M87 is rapidly rotating clockwise with rotation parameter  $a = 0.9 \pm 0.1$  and inclination  $i = 17^\circ$ , equivalent to a magnetic arrested disk with inclination  $i = 163^\circ$ , confirming the relativistic effect discussed in Ref. 5. With our findings we have been able, for the first time, to directly detect and characterize the relativistic properties of the spacetime described by the Kerr metric [25].

We thank Guido Chincarini for help and useful discussions. F. T. acknowledges ZKM and Peter Weibel for the financial support. The encouragement and support from Erik B. Karlsson is gratefully acknowledged.

---

\* Electronic address: [fabrizio.tamburini@gmail.com](mailto:fabrizio.tamburini@gmail.com)

† Electronic address: [bt@irfu.se](mailto:bt@irfu.se)

‡ Electronic address: [massimo.dellavalle@inaf.it](mailto:massimo.dellavalle@inaf.it)

- [1] J. P. Torres and L. Torner, *Twisted Photons: Applications of Light With Orbital Angular Momentum* (Wiley-Vch Verlag, John Wiley and Sons, Weinheim, DE, 2011).
- [2] M. Harwit, Photon orbital angular momentum in astrophysics, *Astrophys. J.* **597**, 1266 (2003).
- [3] B. Thidé, N. M. Elias, II, F. Tamburini, S. M. Mohammadi, and J. T. Mendonça, Applications of electromagnetic OAM in astrophysics and space physics studies, in *Twisted Photons: Applications of Light With Orbital Angular Momentum*, edited by J. P. Torres and L. Torner (Wiley-Vch Verlag, John Wiley and Sons, Weinheim, DE, 2011) Chap. 9, pp. 155–178.
- [4] G. Anzolin, F. Tamburini, A. Bianchini, G. Umbriaco, and C. Barbieri, Optical vortices with starlight, *Astron. Astrophys.* **488**, 1159 (2008).
- [5] F. Tamburini, B. Thidé, G. Molina-Terriza, and G. Anzolin, Twisting of light around rotating black holes, *Nature Phys.* **7**, 195 (2011).
- [6] G. Molina-Terriza, J. P. Torres, and L. Torner, Twisted photons, *Nature Phys.* **3**, 305 (2007).
- [7] EHT Collaboration *et al.*, EHT data products, Online image data (2019), retrieved 13–24 April from <https://eventhorizontelescope.org/for-astronomers/data>.
- [8] EHT Collaboration *et al.*, The shadow of the supermassive black hole, *Astrophys. J. Lett.* **875**, L1(17) (2019), First M87 Event Horizon Telescope Results I.
- [9] EHT Collaboration *et al.*, Array and instrumentation, *Astrophys. J. Lett.* **875**, L2(28) (2019), First M87 Event Horizon Telescope Results II.
- [10] EHT Collaboration *et al.*, Data processing and calibration, *Astrophys. J. Lett.* **875**, L3(32) (2019), First M87 Event Horizon Telescope Results III.
- [11] EHT Collaboration *et al.*, Imaging the central supermassive black hole, *Astrophys. J. Lett.* **875**, L4(52) (2019), First M87 Event Horizon Telescope Results IV.
- [12] EHT Collaboration *et al.*, Physical origin of the asymmetric ring, *Astrophys. J. Lett.* **875**, L5(31) (2019), First M87 Event Horizon Telescope Results V.

- [13] EHT Collaboration *et al.*, The shadow and mass of the central black hole, *Astrophys. J. Lett.* **875**, L6(44) (2019), First M87 Event Horizon Telescope Results VI.
- [14] S. M. Barnett and L. Allen, Orbital angular momentum and nonparaxial light beams, *Opt. Commun.* **110**, 670 (1994).
- [15] L. Torner, J. P. Torres, and S. Carrasco, Digital spiral imaging, *Opt. Express* **13**, 873 (2005).
- [16] C. Bambi, K. Freese, S. Vagnozzi, and L. Visinelli, Testing the rotational nature of the supermassive object M87\* from the circularity and size of its first image, arXiv:1904.12983 [astro-ph, physics:gr-qc] (2019).
- [17] B. Thidé, H. Then, J. Sjöholm, *et al.*, Utilization of photon orbital angular momentum in the low-frequency radio domain, *Phys. Rev. Lett.* **99**, 087701(4) (2007).
- [18] F. Tamburini, E. Mari, B. Thidé, C. Barbieri, and F. Romanato, Experimental verification of photon angular momentum and vorticity with radio techniques, *Appl. Phys. Lett.* **99**, 204102 (2011).
- [19] F. Tamburini, E. Mari, A. Sponselli, B. Thidé, A. Bianchini, and F. Romanato, Encoding many channels on the same frequency through radio vorticity: first experimental test, *New J. Phys.* **14**, 03301 (2012).
- [20] S. Barbero, Error analysis and correction in wavefront reconstruction from the transport-of-intensity equation, *Opt. Express* **45**, 094001 (2006).
- [21] C. Schulze, D. Naidoo, D. Flamm, O. A. Schmidt, A. Forbes, and M. Duparré, Wavefront reconstruction by modal decomposition, *Opt. Express* **20**, 19714 (2012).
- [22] A. Lubk, G. Guzzinati, F. Börrnert, and J. Verbeeck, Transport of intensity phase retrieval of arbitrary wave fields including vortices, *Phys. Rev. Lett.* **111**, 173902 (2013).
- [23] A. Ruelas, S. Lopez-Aguayo, and J. C. Gutiérrez-Vega, Wavefront reconstruction of vortex beams via a simplified transport of intensity equation and its symmetry based error reduction, *J. Opt.* **21**, 015602 (2018).
- [24] D. P. Kelly, Measuring the phase of an optical field from two intensity measurements: Analysis of a simple theoretical model, *Int. J. Opt.* **2018**, 1 (2018).
- [25] R. P. Kerr, Gravitational field of a spinning mass as an example of algebraically special metrics, *Phys. Rev. Lett.* **11**, 237 (1963).
- [26] B. Chen, R. Kantowski, X. Dai, E. Baron, and P. Maddumage, Algorithms and programs for strong gravitational lensing in Kerr space-time including polarization, *Astrophys. J. Suppl. Ser.* **218**, 4 (2015).
- [27] D. Zhang, X. Feng, K. Cui, F. Liu, and Y. Huang, Identifying orbital angular momentum of vectorial vortices with Pancharatnam phase and Stokes parameters, *Sci. Rep.* **5**, 11982 (2015).
- [28] D. N. Sob'yanin, Black hole spin from wobbling and rotation of the M87 jet and a sign of a magnetically arrested disc, *Mon. Not. Roy. Astron. Soc. Lett.* **479**, L65 (2018).
- [29] L. Allen and M. Padgett, The orbital angular momentum of light: An introduction, in *Twisted Photons: Applications of Light With Orbital Angular Momentum*, edited by J. P. Torres and L. Torner (Wiley-Vch Verlag, John Wiley and Sons, Weinheim, DE, 2011) Chap. 1, pp. 1–12.
- [30] B. Thidé, F. Tamburini, H. Then, C. G. Sameda, and R. A. Ravanelli, The physics of angular momentum radio, arXiv:1410.4268 [physics.optics] (2014).
- [31] J. W. Goodman, *Introduction to Fourier Optics*, 3rd ed. (Roberts, Englewood, CO, USA, 1996) p. 528.
- [32] S. S. Doeleman, V. L. Fish, D. E. Schenck, *et al.*, Jet-launching structure resolved near the supermassive black hole in M87, *Science* **338**, 355 (2012).
- [33] D. Christodoulou and R. Ruffini, Reversible transformations of a charged black hole, *Phys. Rev. D* **4**, 3552 (1971).
- [34] A. Doi, K. Hada, H. Nagai, M. Kino, M. Honma, K. Akiyama, T. Oyama, and Y. Kono, ALMA continuum spectrum of the M87 nucleus - quasi-simultaneous continuum observations at bands-3, 6, 7, and 9, *EPJ Web of Conferences* **61**, 08008 (2013).
- [35] G. B. Rybicki and A. P. Lightman, *Radiative Processes in Astrophysics*, Physics Textbook (Wiley, Weinheim, 2004) p. 382.